International Journal of Pharmacology

*Int. J. Pharmacol.* **2026**; 22(3): 48017
https://doi.org/10.31083/IJP48017

*Research Article*

# Network Pharmacology Combined With Experimental Validation Reveals the Mechanism of Action of *Megacarpaea delavayi* on L-arginine-Induced Functional Dyspepsia

Liqi Cang[1,†], Zhongyang Deng[1,†], Hangrao Wang[2], Jie Zhou[2], Jinda Wang[2], Bei Jiang[1,2], Lei Shen[1,2,*]

[1]Yunnan Key Laboratory of Screening and Research on Anti-pathogenic Plant Resources from Western Yunnan, Dali University, 671000 Dali, Yunnan, China
[2]College of Pharmacy, Dali University, 671000 Dali, Yunnan, China
*Correspondence: shenlei@dali.edu.cn (Lei Shen)
[†]These authors contributed equally.

Academic Editor: Mehmet Ozaslan
Submitted: 5 November 2025 Revised: 14 December 2025 Accepted: 17 December 2025 Published: 12 May 2026

**Abstract**

**Background**: This study aimed to evaluate the therapeutic effect of *Megacarpaea delavayi* (*M. delavayi*) on L-arginine (L-arg)-induced functional dyspepsia (FD) and to elucidate the associated underlying mechanisms using network pharmacology and *in vivo* experiments. **Methods**: A mouse model of L-arg-induced FD was established to assess the efficacy of *M. delavayi*. Subsequently, network pharmacology analysis was employed to predict potential candidate targets and signaling pathways of *M. delavayi*. Finally, the candidate targets were assessed in the mouse model described above. **Results**: *M. delavayi* promoted gastrointestinal peristalsis, reduced gastric tissue damage, increased serum levels of motilin (MTL) and gastrin (GAS), and decreased acetylcholinesterase (AChE) level in FD mice. Network pharmacology analysis identified 102 overlapping targets at the intersection of *M. delavayi*-related compounds and FD-associated genes. Protein-protein interaction (PPI) network analysis identified inflammation-associated targets, including interleukin-6 (IL6), tumor necrosis factor (TNF), nitric oxide synthase 1 (NOS1), epidermal growth factor receptor (EGFR), SRC proto-oncogene (SRC), and signal transducer and activator of transcription 3 (STAT3). Integration of these targets with functional and pathway enrichment analyses revealed that nitric oxide (NO) and related inflammatory signaling pathways play a pivotal role in the pharmacological effects of *M. delavayi*. Validation in FD mice further demonstrated that *M. delavayi* decreased $O_2^-$ contents and restored the impaired NO-soluble guanylate cyclase (sGC)-protein kinase G (PKG) signaling pathway by elevating the levels of neuronal nitric oxide synthase (nNOS), sGC and PKG. Conversely, an increase in inducible nitric oxide synthase (iNOS) expression was also observed. **Conclusion**: *M. delavayi* effectively ameliorates L-arg-induced gastrointestinal dysfunction through restoration of the NO-sGC-PKG signaling pathway.

**Keywords:** *Megacarpaea delavayi*; functional dyspepsia; nitric oxide; soluble guanylate cyclase; protein kinase G; network pharmacology

## 1. Introduction

Functional dyspepsia (FD) is a prevalent, chronic, and recurrent gastrointestinal disorder with an estimated prevalence ranging from 10% to 40% in Western countries and 5% to 30% in Asia [1]. It is characterized by symptoms such as epigastric discomfort, bloating, early satiety, belching, nausea, and acid regurgitation, in the absence of detectable organic pathology. Although FD is not a life-threatening disease, it markedly impairs work performance and quality of life, and places a considerable economic burden on individuals and healthcare systems. Current medicines for FD include proton pump inhibitors, prokinetic agents (e.g., domperidone and metoclopramide), antidepressants, and mucosal protectants [2,3]. However, their clinical applications are limited by potential adverse effects, variable efficacy among individuals, and high relapse rates following discontinuation [4,5].

Ethnomedicines are guided by traditional medical theories and supported by long-term clinical practice. Therefore, their application in treating chronic refractory diseases such as FD represents a feasible therapeutic strategy [6]. In Dali, Yunnan province of China, a plant, *Megacarpaea delavayi* (*M. delavayi*) Franchet, has been employed as a traditional ethnic medicine for centuries to treat FD. *M. delavayi*, commonly known as Gaohecai (Chinese name) or Ganlgect (Bai ethnic name), is a perennial herb that belongs to the genus *Megacarpaea* in the Brassicaceae family. It grows in high-altitude regions at elevations between 3400 and 3800 meters. This genus comprises seven species worldwide, three of which are distributed in China, mainly in Yunnan, Sichuan, Gansu, and Tibet. According to traditional medicinal records of the Bai ethnic group, *M. delavayi* is used as both a medicinal and a food plant for treating dysentery, gastric heat accumulation, indigestion, and heat-related cough. Recent pharmacological stud-

ies have demonstrated that *M. delavayi* can promote gastric emptying and small intestinal propulsion in both normal mice and those with FD, enhance contractions of the isolated guinea pig ileum, and stimulate gastric acid secretion in rats with food stagnation [7–9]. However, its comprehensive therapeutic efficacy and underlying mechanisms remain insufficiently elucidated.

Although the pathophysiology of FD remains incompletely understood, several key mechanisms have been proposed, including disordered gastrointestinal motility associated with central modulation, visceral hypersensitivity to mechanical or chemical stimuli, dysregulation of the brain-gut axis, and *Helicobacter pylori* infection [10]. Recently, increasing evidence has revealed the role of nitric oxide (NO) and its related signaling pathway in the regulation of gastrointestinal function. In the gastrointestinal tract, NO is an essential inhibitory neurotransmitter that is biosynthesized through the catalysis of nitric oxide synthase (NOS). Physiologically, NO generated by endothelial NOS (eNOS) or neuronal NOS (nNOS) modulates smooth muscle relaxation via the NO-guanylate cyclase (GC)-protein kinase G (PKG) pathway [11–13]. However, under FD conditions, both the impaired NO synthesis from nNOS dysfunction and abnormal NO release mediated by inducible NOS (iNOS) are closely associated with gastrointestinal dysmotility. Dysregulation of the NO–sGC–PKG signaling pathway may lead to delayed gastric emptying and impaired accommodation, which are key features of FD [14–17]. Excessive intake of L-arginine (L-arg), a metabolic precursor of NO, could lead to overproduction of NO both directly and indirectly, and could further impair gastrointestinal function [18]. Compared with other classical FD animal models, such as those induced by iodoacetamide or tail clamp stimulation, the L-arg model can successfully replicate key clinical features of FD, including delayed gastric emptying and reduced intestinal propulsion, without causing obvious necrosis, erosion, or organic lesions. Thus, this model can closely mimic human FD [19–21].

This study investigated the efficacy of *M. delavayi* in treating FD and explored its underlying mechanism in an L-arg-induced mouse model. These findings may provide a scientific basis for the traditional application of *M. delavayi* in FD treatment.

## 2. Materials and Methods

### *2.1 Experimental Animals*

Male SPF grade ICR mice (18–22 g) were procured from Speforward (Beijing) Biotechnology Co., Ltd. (License No. SCXK (Beijing) 2024-0001). Mice were housed under standard laboratory conditions (18–22 °C, 50–60% relative humidity) with a 12 h light/dark cycle and had ad libitum access to food and water. Animals were acclimatized to the laboratory environment for one week prior to experimentation. All animal procedures were performed in accordance with the guidelines of the Animal Ethics Committee of Dali University (Ethics No. 2024-P2-110).

### *2.2 Experimental Drugs*

The whole plant of *M. delavayi* was collected in Dali City, Yunnan Province, China, and authenticated morphologically by Dr. Yong-Zeng Zhang at the College of Pharmacy, Dali University, Yunnan Province, China. A voucher specimen was deposited at the Yunnan Key Laboratory of Screening and Research on Anti-pathogenic Plant Resources from Western Yunnan, Dali University (plant sample preservation number: 20180627-4). Two kilograms of plant samples were milled and extracted three times with 95% ethanol at room temperature (24 h, 48 h, and 48 h, respectively). The resulting extracts were combined, filtered, and concentrated under reduced pressure using a rotary evaporator, yielding 445 g of freeze-dried powder. Prior to administration, the powders were suspended in a 0.5% CMC-Na solution. CMC-Na (Batch No: IS9000) was purchased from Solarbio Biotechnology Co., Ltd., Beijing, China. Domperidone was purchased from Shanghai Yuan-Ye Co., Ltd. (Batch No: S26612) and used as a positive control drug.

### *2.3 Experimental Reagents*

L-arg (Batch No: 150905) and superoxide anion ($O_2^-$) detection kit (Batch No: BC1290) were purchased from Solarbio Biotechnology Co., Ltd., China. Evans Blue dye (Batch No. 991107) was purchased from the Shanghai Chemical Reagents Procurement and Supply Station. Detection kits of motilin (MTL, Batch No: H182-1-2) and gastrin (GAS, Batch No: H239-1-2) were sourced from Nanjing Jiancheng Bioengineering Co., Ltd., China. Detection kits of vasoactive intestinal peptide (VIP, Batch No: E-EL-M1234) and acetylcholinesterase (AChE, Batch No: E-EL-M26) were purchased from Elabscience Biotechnology Co., Ltd., China. Detection kits of soluble guanylate cyclase (sGC, Batch No: ml925127V), protein kinase G (PKG, Batch No: ml037829V), inducible nitric oxide synthase (iNOS, Batch No: ml057773V), and neuronal nitric oxide synthase (nNOS, Batch No: ml0930900) were sourced from Shanghai Enzyme-linked Biotechnology Co., Ltd., China. The primary antibodies against sGC (Batch No: 19011-1-AP), PKG (Batch No: 21646-1-AP), nNOS (Batch No: 29231-1-AP), iNOS (Batch No: 22226-1-AP), and $\beta$-actin (Batch No: 20536-1-AP), as well as the horseradish peroxidase (HRP)-linked secondary antibody (Batch No: RGAR001, 1:6000), were purchased from Proteintech Group, Inc., China.

### *2.4 Functional Dyspepsia (FD) Model Establishment, Animal Grouping and Administration*

After acclimation, sixty mice were randomly assigned to six groups (n = 10 per group): control, model, domperi-

done (0.1 g/kg, positive control), and *M. delavayi* extract (1.0, 0.5, and 0.25 g/kg). All treatments were administered once daily by gavage for 7 days at an administration volume of 20 mL/kg. From days 4–7, all mice except those in the control group received L-arg (3 g/kg, 1 h before drug treatment) intragastrically to induce FD. The dosage and administration period were determined based on preliminary experiments and previously published studies.

### *2.5 Assessment of Gastric Emptying Rate and Intestinal Propulsion Rate*

A blue-colored semi-solid nutritional paste (300 mL) was prepared by dissolving 10 g sodium carboxymethyl cellulose in 250 mL distilled water, followed by sequential addition of 12 g sucrose, 16 g milk powder, and 10 g starch to form a suspension under continuous stirring, with the final addition of 0.1 g Evans Blue dye as a visual tracer. The paste was stored at 4 °C and warmed to room temperature prior to oral administration. After seven days of administration, mice were for fasted 12 h with ad libitum access to water. The next morning, each mouse was administered 0.8 mL of the prepared paste through gavage. Twenty minutes post-gavage, the blood of each mouse was collected. Following collection, mice were euthanized by cervical dislocation, and their abdomen was excised. After ligation of both the cardia and pylorus, the entire stomach was removed and rinsed with saline to eliminate blood contaminants. The total weight of stomach was weighed, then the stomach was opened along the greater curvature, and the gastric contents were washed with saline. The emptied stomach was wiped dry with filter paper before measurement of the net weight of the stomach. Gastric emptying rate (%) was calculated as: [Weight of administered paste – (total weight of stomach – net weight of stomach)] / Weight of administered paste × 100%. Concurrently with stomach isolation, the entire small intestine was excised from the distal pylorus to the ileocecal junction. Both the total length of the small intestine and the propulsion distance of the paste were measured to calculate intestinal propulsion rate (%) as: Propulsion distance of the paste / Total length of the small intestine × 100%.

### *2.6 Sample Collection*

Blood samples were collected from the retro-orbital plexus under brief isoflurane (3% for induction and 1.5–2% for maintenance, administered via inhalation using a calibrated vaporizer with oxygen flow) anesthesia and allowed to stay at room temperature for 2 h. Then, serum was prepared by centrifugation (3000 rpm for 10 min) at 4 °C, stored at –80 °C, and used to analyze the levels of gastrointestinal hormone. The gastric antrum specimen was isolated from the stomach and fixed in 4% paraformaldehyde for histopathological examination. The ileum tissue was obtained from the small intestine and homogenised on ice for subsequent analysis, including Enzyme-Linked Immunosorbent Assay (ELISA) and WB.

### *2.7 Hematoxylin and Eosin (H&E) Staining*

Following fixation, gastric specimens were processed through standard H&E staining protocols, including paraffin embedding, sectioning, xylene dewaxing, graded ethanol rehydration, H&E staining, ethanol dehydration, xylene clearing, and neutral balsam mounting. Histopathological changes were observed under a light microscope.

### *2.8 ELISA*

ELISA kits were employed to quantify the levels of gastrointestinal hormones and the contents of the key NO-sGC-PKG signaling pathway components in mice. After the preparation of serum, the contents of MTL, GAS, VIP, and AChE were measured according to the kit protocols. The samples of ileum tissues were homogenized and centrifuged, and the resulting supernatant was used to measure the contents of sGC, PKG, nNOS, iNOS and $O_2^-$ with the kit instructions.

### *2.9 Western Blot*

Ileal tissues were lysed in high-efficiency RIPA lysis buffer (Solarbio, Beijing, China; Batch No. 20220211) supplemented with a 50× protease–phosphatase inhibitor cocktail (Beyotime Biotechnology, Shanghai, China; Batch No. 020221210218). Protein concentrations were determined using a BCA protein assay kit (Biosharp Biotechnology Co., Ltd., China; Batch No. 21362908). Equal amounts of protein were resolved by SDS–PAGE and transferred onto polyvinylidene fluoride (PVDF) membranes (Millipore, Germany; Batch No. R1AB03348) using a Mini Trans-Blot transfer system (Bio-Rad, Hercules, CA, USA). Membranes were blocked with 5% non-fat dry milk (Solarbio, Beijing, China; Batch No. 107B053) for 1 h at room temperature and then incubated overnight at 4 °C with primary antibodies against sGC (1:4000), PKG (1:3000), nNOS (1:4000), iNOS (1:1000), and $\beta$-actin (1:6000) (Proteintech Group, Wuhan, China). After three washes with TBST, membranes were incubated with HRP-conjugated secondary antibodies (goat anti-rabbit IgG, Proteintech) for 2 h at room temperature. Protein bands were visualized using an ultrasensitive ECL chemiluminescence detection kit (Beyotime Biotechnology, Shanghai, China; Batch No. 090921220310) and imaged with a ChemiDoc XRS+ system (Bio-Rad, USA). Relative protein levels were normalized to $\beta$-actin.

### *2.10 Network Pharmacology*

A total of 49 compounds isolated from the 95% ethanol extract of *M. delavayi* (as reported by Tang [22]) were subjected to network pharmacology analysis. Potential molecular targets of the identified compounds were predicted using the SwissTargetPrediction database (http://www.swisstargetprediction.ch/), and targets with a probability >0.15 were retained for further analysis. FD-related genes were retrieved from the GeneCards database and sub-

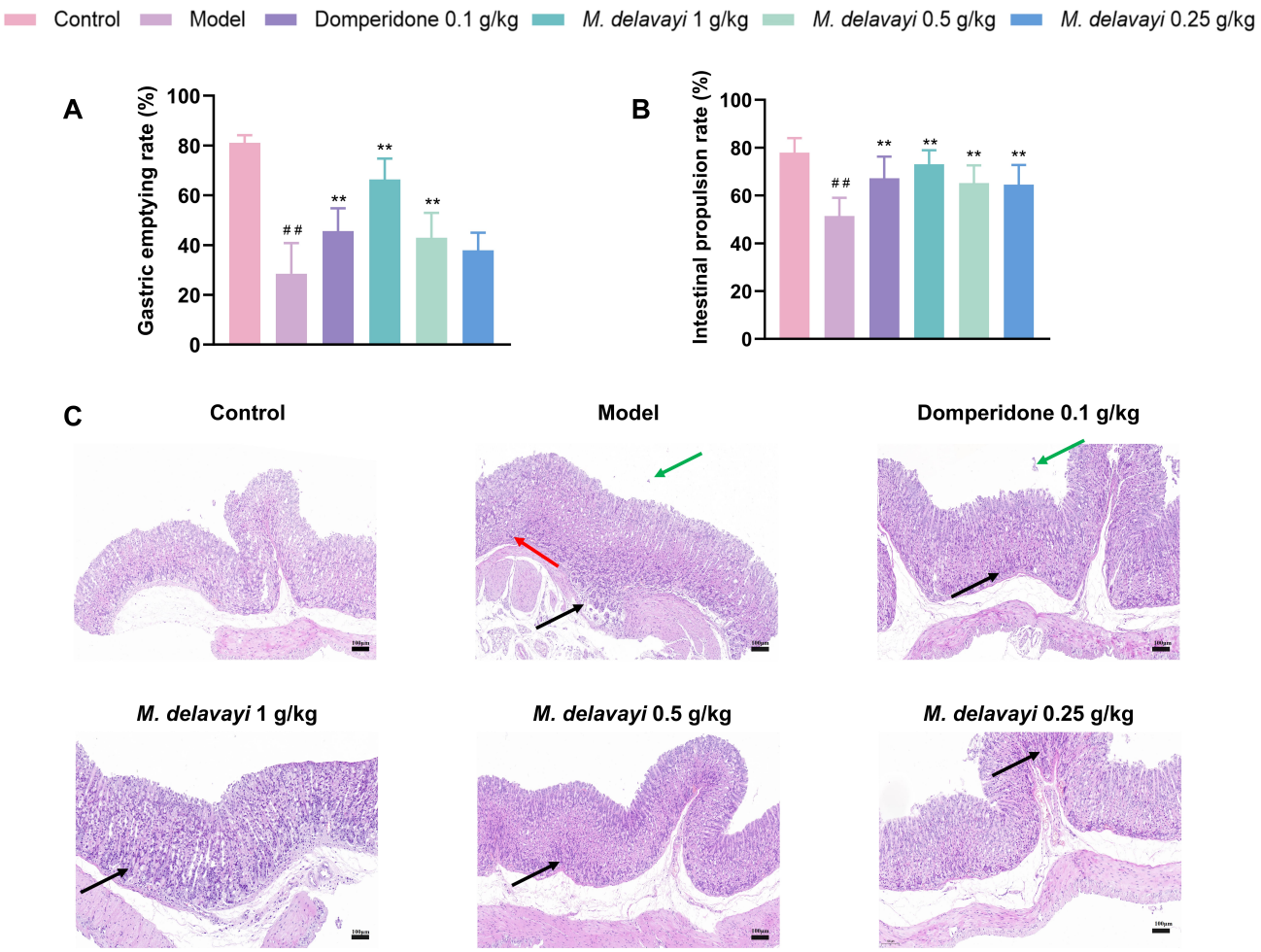


**Fig. 1. Effect of *M. delavayi* on gastrointestinal motility and gastric tissue damage in FD mice.** (A) Gastric emptying rate (n = 10). (B) Small intestinal propulsion rate (n = 10). $^{\#\#}p < 0.01$ vs. the control, $^{**}p < 0.01$ vs. the model. (C) H&E staining images of gastric antrum tissue (scale bar = 100 μm). Green arrows indicate desquamation of epithelial cells, red arrow indicates focal necrosis of gastric glandular cells, and black arrows indicate infiltration of inflammatory cells. Data are presented as mean ± SD. *M. delavayi*, *Megacarpaea delavayi*; FD, functional dyspepsia; H&E, Hematoxylin and Eosin.

sequently refined through additional screening via OMIM and DisGeNET databases. The overlapping targets between *M. delavayi* compounds and FD-related genes were identified through a Venn diagram using the Jvenn online platform. These targets were regarded as potential candidates for *M. delavayi* in treating FD and imported into the STRING database (https://string-db.org/) to construct a protein-protein interaction (PPI) network, with parameters set to *Homo sapiens* species and a minimum interaction confidence score of 0.7. The PPI results were visualized and topologically analyzed using Cytoscape 3.9.1 software. The key nodes were selected based on the median centrality (betweenness), proximity to centrality (closeness), and degree of freedom (degree). Subsequently, the analysis of Gene Ontology (GO) function enrichment and Kyoto Encyclopedia of Genes and Genomes (KEGG) pathway enrichment were performed using the DAVID functional annotation tool. Hierarchical clustering heatmaps and bubble plots were generated to visualize the enriched pathways, with statistical significance set at $p < 0.05$.

### *2.11 Statistical Analysis*

Data were presented as mean ± standard deviation (SD). Statistical analysis was performed using GraphPad Prism 10.0 (GraphPad Software, San Diego, CA, USA), with one-way analysis of variance (ANOVA) followed by post hoc tests for multiple group comparisons. Tukey's test was used for uniform variance, while the Dunnett's T3 test was applied for non-uniform variance. $p < 0.05$ was considered statistically significant.

## 3. Results

### *3.1 Effect of M. delavayi on Gastrointestinal Motility and Gastric Tissue Damage in FD Mice*

Compared to the control group, L-arg administration significantly reduced gastric emptying rate and intestinal

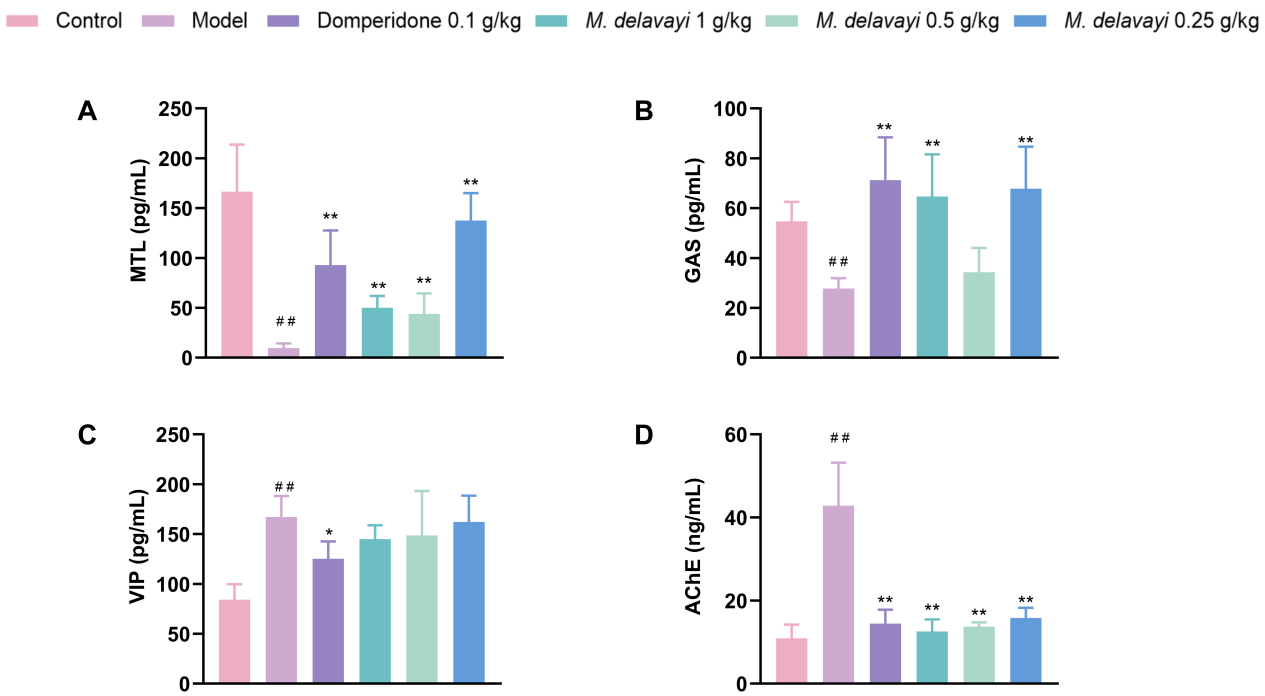


**Fig. 2. Effect of *M. delavayi* on serum levels of gastrointestinal hormones and AChE in FD mice (n = 6).** (A) MTL level. (B) GAS level. (C) VIP level. (D) AChE level. $^{\#\#}p < 0.01$ vs. the control, $^{**}p < 0.01$, $^{*}p < 0.05$ vs. the model. MTL, motilin; GAS, gastrin; VIP, vasoactive intestinal peptide; AChE, acetylcholinesterase. Data are presented as mean ± SD.

propulsion rate, both of which are key indicators of abnormal gastrointestinal motility observed in the model group ($p < 0.01$) (Fig. 1A,B). As expected, both the positive drug domperidone and *M. delavayi* treatment markedly restored gastric emptying rate and small intestinal propulsion rate compared to the model group ($p < 0.01$) (Fig. 1A,B), except for the 0.25 g/kg *M. delavayi*, which had no obvious effect on gastric emptying rate. These findings indicate that *M. delavayi* alleviates FD symptoms by promoting gastrointestinal peristalsis.

In the control group, H&E staining of the gastric antrum tissue exhibited uniformly stained cells and orderly arranged muscle fibers in the muscularis layer. The lamina propria contained abundant gastric glands with intact morphology. There were no obvious pathological alterations or inflammatory cell infiltration observed (Fig. 1C). In contrast, the model group displayed gastric tissue abnormalities, including desquamation of epithelial cells (green arrows) and focal necrosis of gastric glandular cells (red arrows, pyknotic nuclei) in the lamina propria, and marked infiltration of inflammatory cells (black arrows) in the submucosal layer (Fig. 1C). After domperidone and *M. delavayi* treatment, gastric antrum tissue exhibited varying degrees of improvement in structure, with relatively preserved epithelial integrity and reduced inflammatory infiltration (Fig. 1C).

### *3.2 Effect of M. delavayi on Serum Levels of Gastrointestinal Hormone in FD Mice*

Gastrointestinal hormones play important roles in regulating gastric motility and peristaltic rhythm. Compared to the control group, serum levels of motilin MTL and GAS were significantly reduced in the model group ($p < 0.01$) (Fig. 2A,B), while levels of VIP and AChE were markedly elevated ($p < 0.01$) (Fig. 2C,D). After drug intervention, compared with the model group, *M. delavayi* at 0.25, 0.5, and 1 g/kg, as well as domperidone, significantly increased MTL and GAS levels ($p < 0.01$) (Fig. 2A,B), except for the 0.5 g/kg *M. delavayi*, which showed no significant effect on GAS. All the treatments also exhibited marked suppression of AChE activity ($p < 0.01$) (Fig. 2D), leading to elevated ACh levels. Notably, VIP levels remained unchanged in all *M. delavayi* treatment groups ($p > 0.05$); only a significant decrease in VIP levels was observed in the domperidone group ($p < 0.05$) (Fig. 2C). These results demonstrate that *M. delavayi* ameliorates impaired gastrointestinal motility in FD mice by restoring physiological levels of excitatory gastrointestinal hormones (MTL, GAS, and ACh).

### *3.3 Network Pharmacology Prediction*

Based on previous phytochemical investigations, 49 active compounds were identified from *M. delavayi*. Among these, 35 compounds (**Supplementary Table 1**) were predicted to have corresponding protein targets. After

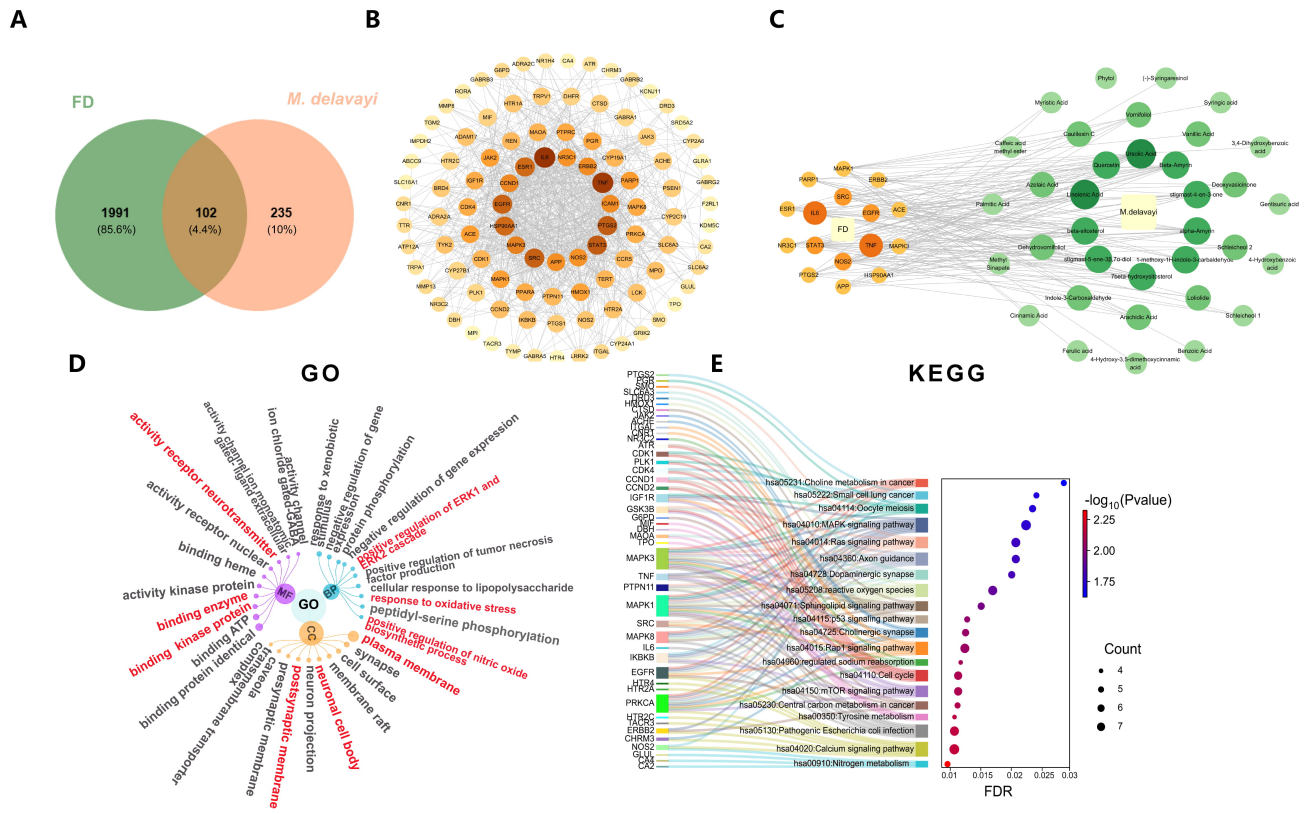


**Fig. 3. Network pharmacology prediction.** (A) Venn diagram of overlapping target genes between FD and *M. delavayi*. (B) PPI network visualization of the total of 102 overlapping target genes. (C) PPI network visualization of the top 16 targets and their corresponding compounds in *M. delavayi*. (D) Hierarchical network plot for GO enrichment analysis (top 10 items). (E) Sankey diagram (left) and bubble plot (right) for KEGG enrichment analysis (top 20 items). BP, biological process; MF, molecular function; CC, cellular component; KEGG, Kyoto Encyclopedia of Genes and Genomes.

target prediction using the SwissTargetPrediction database and removal of duplicate targets, 337 potential protein targets were obtained. Meanwhile, 2093 FD-associated genes were retrieved from three databases. Comparative analysis of compound-related targets and disease-associated genes yielded 102 overlapping targets, which were visualized in a Venn diagram (Fig. 3A).

The PPI network of the 102 overlapping targets was analyzed using the STRING database and constructed using Cytoscape software. The network consisted of 102 nodes and 847 edges, with an average node degree of 6.48 (Fig. 3B). These targets were further filtered and explored through PPI network analysis, leading to the identification of 16 core targets. Among these, six are associated with inflammation, including IL6, TNF, NOS1, EGFR, SRC, and STAT3 (Fig. 3C).

GO enrichment analysis was performed across the categories of biological process (BP), molecular function (MF), and cellular component (CC), using a significance threshold of $p < 0.05$ with false discovery rate correction ($q < 0.05$) (Fig. 3D). The top 10 enriched GO entries were visualized using a hierarchical network plot (Fig. 3D). Notable BP mainly involved positive regulation of the ERK1/2 cascade, response to oxidative stress, and positive regulation of the NO biosynthetic process. The CC mainly included the plasma membrane, neuronal cell body, and postsynaptic membrane. The MF primarily involved protein kinase binding, enzyme binding, and neurotransmitter receptor activity.

KEGG pathway enrichment analysis identified 120 enriched entries, and the top 20 significantly enriched signaling pathways were visualized using a bubble plot (Fig. 3E). The results demonstrated that the nitrogen metabolism, calcium signaling pathway, cholinergic synapse, and reactive oxygen species (ROS) were the main enriched pathways.

Integration of the core targets with GO and KEGG enrichment analysis revealed that NO and its associated inflammatory signaling pathways play a pivotal role in the action of *M. delavayi*, requiring further validation.

### *3.4 Effect of M. delavayi on the NO-sGC-PKG Signaling Pathway in FD Mice*

Firstly, the ELISA assay was used to quantify the levels of key components in the NO-sGC-PKG signaling pathway, which is closely associated with neurotransmitter re-

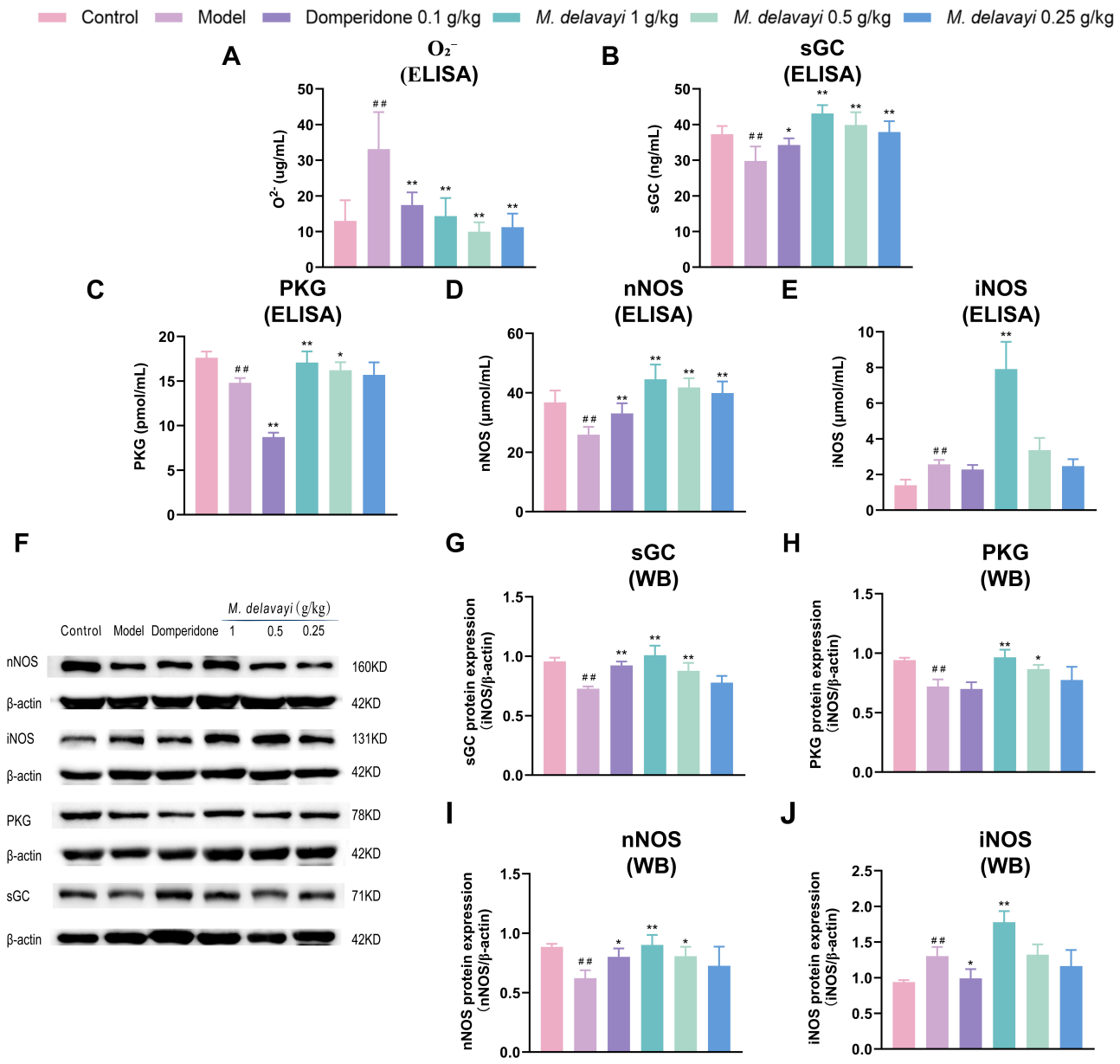


**Fig. 4. Effect of *M. delavayi* on the NO-sGC-PKG signaling pathway in FD mice.** (A–E) The levels of $O_2^-$, sGC, PKG, nNOS, and iNOS were measured by ELISA (n = 8). (F) Western Blot image. (G–J) The relative protein levels of sGC, PKG, nNOS, and iNOS were measured by Western Blot (n = 4). $^{\#\#}p < 0.01$ vs. the control, $^{**}p < 0.01$, $^{*}p < 0.05$ vs. the model. $O_2^-$, superoxide anion; sGC, soluble guanylate cyclase; PKG, protein kinase G; nNOS, neuronal nitric oxide synthase; iNOS, inducible nitric oxide synthase. Data are presented as mean ± SD.

ceptor modulation, inflammatory responses, and oxidative stress regulation. Compared to the normal group, L-arg intervention in FD mice significantly elevated $O_2^-$ contents ($p < 0.01$, Fig. 4A) and suppressed levels of sGC and PKG ($p < 0.01$, Fig. 4B,C) in intestinal tissues, while differentially modulated the contents of NOS isoforms by inhibiting nNOS expression ($p < 0.01$, Fig. 4D) but enhancing iNOS content ($p < 0.01$, Fig. 4E). Similar results were observed by WB analysis (Fig. 4F).Administration of *M. delavayi* at all doses ameliorated L-arg-induced abnormal activities of the NO-sGC-PKG signaling pathway in a dose-dependent manner. Specifically, all dose of *M. delavayi* (1, 0.5, and 0.25 g/kg) obviously decreased $O_2^-$ contents ($p < 0.01$, Fig. 4A) and elevated the levels of sGC and nNOS ($p < 0.01$, Fig. 4B,D). Only the 1 and 0.5 g/kg *M. delavayi* markedly increased PKG level ($p < 0.01$ or $p < 0.05$, Fig. 4C). The 0.5 and 0.25 g/kg *M. delavayi* did not significantly alter iNOS levels ($p > 0.05$, Fig. 4E), whereas the 1.0 g/kg dose unexpectedly induced a pronounced elevation of iNOS ($p < 0.01$, Fig. 4E), suggesting a dose-dependent but complex regulatory effect on iNOS synthesis.

Similar results were observed by WB analysis. Compared to the model group, 1 and 0.5 g/kg *M. delavayi* significantly increased the protein expression levels of sGC, PKG, and nNOS ($p < 0.01$ or $p < 0.05$, Fig. 4G–I). Meanwhile, 0.5 and 0.25 g/kg *M. delavayi* had no significant effect on iNOS expression ($p > 0.05$, Fig. 4J), whereas 1 g/kg *M. delavayi* markedly upregulated iNOS protein levels ($p < 0.01$, Fig. 4J).

## 4. Discussion

As a traditional medicine and food plant, *M. delavayi* has long been used by the Bai people in Dali of China to treat FD. However, modern pharmacological evidence supporting its efficacy is still inadequate. Here, our results demonstrate that *M. delavayi* effectively improves gastrointestinal motility in an L-arg-induced FD mouse model, which closely mimics the human disease. These findings are consistent with the ethnomedicinal use of *M. delavayi* by local populations, where it has been consumed to enhance appetite, strengthen the spleen, and relieve indigestion, thus providing experimental support for its traditional application.

Gastrointestinal motility is modulated by the autonomic and enteric nervous systems (ANS and ENS), as well as various gastrointestinal hormones, including MTL, GAS, and VIP. MTL and GAS promote gastric emptying, gastric acid secretion, and mucosal growth, whereas VIP induces smooth muscle relaxation via vasoactive intestinal polypeptide receptor activation and myosin light chain kinase inhibition [23,24]. These hormones function in a coordinated and dynamic manner to fine-tune gastric accommodation, peristaltic rhythm, and pyloric relaxation, thereby maintaining physiological gastrointestinal motility. Disruption of neural regulation and gastrointestinal hormone secretion can lead to FD. In the L-arg-induced FD model, reduced levels of MTL and GAS contribute to delayed gastric emptying, whereas impaired NO-mediated inhibitory signaling may trigger compensatory upregulation of VIP by the ENS to maintain smooth muscle relaxation and prevent hypercontractility [25]. Such compensatory hormonal alterations reflect an adaptive response of the ENS to disturbed nitrergic signaling; however, persistent imbalance may further aggravate dysmotility and impair coordinated gastrointestinal movement. Our findings indicate that *M. delavayi* extract restores gastrointestinal function by elevating the levels of MTL and GAS and reducing abnormally elevated VIP level, thereby improving gastric emptying, intestinal propulsion, and motility rhythm. In addition to hormonal regulation, cholinergic signaling plays a crucial role in smooth muscle activity, where ACh mediates muscular contraction via the M3 receptor [26]. In the FD model, excessive L-arg intake disrupts physiological NO signaling and is associated with reduced nNOS activity, thereby impairing normal NO synthesis [27]. This diminishment of inhibitory tone weakens the control of cholinergic neurons, ultimately eliciting compensatory cholinergic hyperactivity characterized by increased ACh release and upregulated AChE activity [28,29]. Here, *M. delavayi* alleviates these cholinergic abnormalities by inhibiting AChE overactivity. Collectively, these results suggest that *M. delavayi* exerts multiple regulatory effects on neurohormonal and neurotransmitter pathways, providing mechanistic insight into its therapeutic potential for FD.

Network pharmacology was utilized to systematically identify bioactive components, therapeutic targets, and enriched pathways associated with *M. delavayi*. GO and KEGG enrichment analyses revealed strong associations with NO biosynthesis, oxidative stress regulation, inflammatory signaling, and calcium homeostasis. Physiologically, NO produced by NOS diffuses into smooth muscle or interstitial cells of Cajal, activates sGC, increases cGMP, and stimulates PKG, thereby reducing intracellular $Ca^{2+}$ levels and suppressing pro-inflammatory cytokines such as IL-6 and TNF-$\alpha$ [30–32]. However, pathological iNOS-derived NO may disrupt this pathway by reacting with ROS (notably $O_2^-$) to generate $ONOO^-$, decreasing NO bioavailability and contributing to mucosal injury and FD progression [33,34]. This reaction depletes physiological NO bioavailability, suppresses nNOS activity, and further promotes iNOS expression [35,36]. Six inflammation-associated targets among the core targets, including IL6, TNF, NOS1, EGFR, SRC, and STAT3, were closely associated with these mechanisms, supporting the involvement of the NO–sGC–PKG signaling pathway in mediating the therapeutic effects of *M. delavayi*. Furthermore, since the present FD model was established using L-arg, tthe NO–sGC–PKG signaling pathway was selected for experimental validation of the plant's mechanism.

The signaling pathway predicted by network pharmacology was further validated using ELISA assay and WB analysis. Our results demonstrate *M. delavayi* restores the function of the NO–sGC–PKG signaling pathway by elevating nNOS activity to recover NO levels, thereby increasing the levels of sGC and PKG to exert antioxidant effects through the scavenging of free radicals and inhibition of lipid peroxidation. Oxidative stress can oxidize the heme group of sGC from the ferrous to the ferric state or induce heme dissociation, markedly impairing sGC responsiveness to NO. Such disruption compromises smooth muscle relaxation, anti-inflammatory responses, and mucosal barrier integrity [37,38]. *M. delavayi* may recover sGC activity through multiple mechanisms, including free radical scavenging, enhancement of NOS-mediated NO production, and reversal of sGC heme oxidation [39–41]. Then, the effect of *M. delavayi* on sGC could elevate cGMP level and reactivate PKG and downstream effectors. Unexpectedly, high-dose *M. delavayi* markedly increased iNOS expression, which may reflect a compensatory or context-dependent regulatory response rather than a purely pathogenic effect. Several mechanisms, includ-

ing compensatory feedback to altered NO–ROS coupling or activation of transcriptional pathways known to regulate iNOS expression, may contribute to this response. However, these remain speculative and require further experimental verification. Importantly, *M. delavayi* simultaneously reduced $O_2^-$ levels, thereby limiting the formation of $ONOO^-$ and diverting NO from pathological nitrative reactions toward physiological NO–sGC–PKG signaling pathway. Collectively, these effects contribute to cytoprotective outcomes. Moreover, previous reports indicate that polysaccharides derived from *M. delavayi* roots can activate NF-$\kappa$B and MAPK pathways and subsequently enhance iNOS transcription [42,43]. The high-dose extract used in the present study may contain elevated levels of these polysaccharides, potentially contributing to the observed iNOS upregulation [44]. Nevertheless, the precise biological significance of iNOS upregulation requires further mechanistic investigation.

## 5. Limitations

This study has several limitations. First, the findings are based on an L-arginine-induced mouse model, which may not fully represent the complexity of human functional dyspepsia. Second, although multiple targets and pathways were predicted by network pharmacology, only the NO–sGC–PKG signaling pathway was experimentally validated. Finally, the specific active compounds of *M. delavayi* responsible for the observed effects were not identified. Future studies, including clinical validation and component-level analysis, are needed to confirm these findings.

## 6. Conclusions

In summary, *M. delavayi* effectively ameliorates L-arg-induced gastrointestinal dysfunction through a multifaceted mechanism involving the regulation of gastrointestinal hormone secretion, restoration of the NO-sGC-PKG signaling pathway, and maintenance of redox homeostasis.

## Availability of Data and Materials

The datasets used and analyzed during the current study are available from the corresponding author on reasonable request.

## Author Contributions

LS and BJ designed the research study. LC, ZD, HW and JZ performed the research. BJ and LS provided guidance on experimental procedures. JW, LC and ZD conducted data analysis and visualization. LC, and ZD developed the methodology. LS and BJ acquired funding. LC and ZD drafted the original manuscript. JW, HW and JZ conducted literature search and reference collection. LC and ZD reviewed and edited the manuscript. All authors contributed to editorial changes in the manuscript. All authors read and approved the final manuscript. All authors have participated sufficiently in the work and agreed to be accountable for all aspects of the work.

## Ethics Approval and Consent to Participate

All animal experiments were conducted in accordance with the approved protocols and guidelines of the Animal Ethics Committee of Dali University (Ethics No. 2024-P2-110). All animal euthanasia procedures were performed in accordance with the AVMA Guidelines for the Euthanasia of Animals.


## Acknowledgment

We extend our heartfelt gratitude to all participants, researchers, technicians, and reviewers who contributed to this study. Their invaluable support and contributions have been instrumental in the successful completion of this research.

## Funding

This research received no external funding.


## Conflict of Interest

The authors declare no conflict of interest.

## Supplementary Material

Supplementary material associated with this article can be found, in the online version, at https://doi.org/10.31083/IJP48017.

## References


[1] Oshima T. Functional Dyspepsia: Current Understanding and Future Perspective. Digestion. 2024; 105: 26–33. https://doi.org/10.1159/000532082.

[2] Miwa H, Nagahara A, Asakawa A, Arai M, Oshima T, Kasugai K, *et al*. Evidence-based clinical practice guidelines for functional dyspepsia 2021. Journal of Gastroenterology. 2022; 57: 47–61. https://doi.org/10.1007/s00535-021-01843-7.

[3] Black CJ, Paine PA, Agrawal A, Aziz I, Eugenicos MP, Houghton LA, *et al*. British Society of Gastroenterology guidelines on the management of functional dyspepsia. Gut. 2022; 71: 1697–1723. https://doi.org/10.1136/gutjnl-2022-327737.

[4] Wauters L, Dickman R, Drug V, Mulak A, Serra J, Enck P, *et al*. United European Gastroenterology (UEG) and European Society for Neurogastroenterology and Motility (ESNM) consensus on functional dyspepsia. United European Gastroenterology Journal. 2021; 9: 307–331. https://doi.org/10.1002/ueg2.12061.

[5] Broeders BWLCM, Carbone F, Balsiger LM, Schol J, Raymenants K, Huang I, *et al*. Review article: Functional dyspepsia-a gastric disorder, a duodenal disorder or a combination of both? Alimentary Pharmacology & Therapeutics. 2023; 57: 851–860. https://doi.org/10.1111/apt.17414.

[6] Coals PGR, Williams VL, Benítez G, Chassagne F, Leonti M. Ethnopharmacology, ethnomedicine, and wildlife conservation. Journal of Ethnopharmacology. 2024; 333: 118399. https://doi.org/10.1016/j.jep.2024.118399.

[7] Fang CS, Wang CJ, Li H. Effects of Megacarpaea delavayi on

Animal Gastrointestinal Motility Function. Yunnan Journal of Traditional Chinese Medicine and Materia Medica. 2006: 52. https://doi.org/10.16254/j.cnki.53-1120/r.2006.03.044. (In Chinese)

[8] Shen L, Fang CS, Wang J, Sa LY, Yang L. Effects of Extracts from Megacarpaea delavayi on Intestinal Propulsion and Gastric Emptying in Mice. Journal of Dali University. 2009; 8: 8–10. (In Chinese)

[9] Shen L, Liu XB, Shi GR, Yang Y, Li B. Effects of Megacarpaea delavayi Extracts on Digestive Juice Components in Rats with Food Stagnation Transforming into Heat Syndrome. Chinese Journal of Ethnomedicine and Ethnopharmacy. 2009; 18: 1–3. (In Chinese)

[10] Singh R, Zogg H, Ghoshal UC, Ro S. Current Treatment Options and Therapeutic Insights for Gastrointestinal Dysmotility and Functional Gastrointestinal Disorders. Frontiers in Pharmacology. 2022; 13: 808195. https://doi.org/10.3389/fphar.2022.808195.

[11] Tenopoulou M, Doulias PT. Endothelial nitric oxide synthase-derived nitric oxide in the regulation of metabolism. F1000Research. 2020; 9: F1000 Faculty Rev–1190. https://doi.org/10.12688/f1000research.19998.1.

[12] Idrizaj E, Traini C, Vannucchi MG, Baccari MC. Nitric Oxide: From Gastric Motility to Gastric Dysmotility. International Journal of Molecular Sciences. 2021; 22: 9990. https://doi.org/10.3390/ijms22189990.

[13] Wang Z, Jin A, Yang Z, Huang W. Advanced Nitric Oxide Generating Nanomedicine for Therapeutic Applications. ACS Nano. 2023; 17: 8935–8965. https://doi.org/10.1021/acsnano.3c02303.

[14] Farahani A, Farahani A, Kashfi K, Ghasemi A. Inducible nitric oxide synthase (iNOS): More than an inducible enzyme? Rethinking the classification of NOS isoforms. Pharmacological Research. 2025; 216: 107781. https://doi.org/10.1016/j.phrs.2025.107781.

[15] Cinelli MA, Do HT, Miley GP, Silverman RB. Inducible nitric oxide synthase: Regulation, structure, and inhibition. Medicinal Research Reviews. 2020; 40: 158–189. https://doi.org/10.1002/med.21599.

[16] Baranipour S, Amini Kadijani A, Qujeq D, Shahrokh S, Haghazali M, Mirzaei A, *et al*. Inducible nitric oxide synthase as a potential blood-based biomarker in inflammatory bowel diseases. Gastroenterology and Hepatology from Bed to Bench. 2018; 11: S124–S128.

[17] da Silva CBP, Ceron CS, Mendes AS, de Martinis BS, Castro MM, Tirapelli CR. Inducible nitric oxide synthase (iNOS) mediates ethanol-induced redox imbalance and upregulation of inflammatory cytokines in the kidney. Canadian Journal of Physiology and Pharmacology. 2021; 99: 1016–1025. https://doi.org/10.1139/cjpp-2021-0108.

[18] Özenver N, Efferth T. Small molecule inhibitors and stimulators of inducible nitric oxide synthase in cancer cells from natural origin (phytochemicals, marine compounds, antibiotics). Biochemical Pharmacology. 2020; 176: 113792. https://doi.org/10.1016/j.bcp.2020.113792.

[19] Bai Y, Liu F, Wan Y, Wu X, Luo S, Zhang L, *et al*. Network pharmacology combined with experimental validation reveals the mechanism of action of erpixing granules on functional dyspepsia. Journal of Ethnopharmacology. 2024; 334: 118553. https://doi.org/10.1016/j.jep.2024.118553.

[20] Liu X, Yang K, Jia Y, Yeertai Y, Wu C, Wang X, *et al*. Chaihushugan powder regulates the gut microbiota to alleviate mitochondrial oxidative stress in the gastric tissues of rats with functional dyspepsia. Frontiers in Immunology. 2025; 16: 1549554. https://doi.org/10.3389/fimmu.2025.1549554.

[21] Zhang J, Wang X, Wang F, Tang X. Xiangsha Liujunzi Decoction improves gastrointestinal motility in functional dyspepsia with spleen deficiency syndrome by restoring mitochondrial quality control homeostasis. Phytomedicine: International Journal of Phytotherapy and Phytopharmacology. 2022; 105: 154374. https://doi.org/10.1016/j.phymed.2022.154374.

[22] Tang YJ. Study on the Chemical Constituents and Anti-malarial Activity of Megacarpaea delavayi [Master's Thesis]. Dali University: Dali. 2024. (In Chinese)

[23] Tait C, Sayuk GS. The Brain-Gut-Microbiotal Axis: A framework for understanding functional GI illness and their therapeutic interventions. European Journal of Internal Medicine. 2021; 84: 1–9. https://doi.org/10.1016/j.ejim.2020.12.023.

[24] Mengting L, Tao LI, Fuhao C, Yan C, Ni L, Yuan Z, *et al*. Weichang' an pill alleviates functional dyspepsia through modulating brain-gut peptides and gut microbiota. Journal of Traditional Chinese Medicine = Chung i Tsa Chih Ying Wen Pan. 2024; 44: 1177–1186. https://doi.org/10.19852/j.cnki.jtcm.2024.06.006.

[25] Wang S, Yan M, Guo Y, Sun R, Jin H, Gong Y. *In vivo* and *in vitro* effects of *Salsola collina* on gastrointestinal motility in rats. Iranian Journal of Basic Medical Sciences. 2020; 23: 383–389. https://doi.org/10.22038/IJBMS.2019.40613.9605.

[26] Takahashi T, Shiraishi A, Murata J, Matsubara S, Nakaoka S, Kirimoto S, *et al*. Muscarinic receptor M3 contributes to intestinal stem cell maintenance via EphB/ephrin-B signaling. Life Science Alliance. 2021; 4: e202000962. https://doi.org/10.26508/lsa.202000962.

[27] Sanders KM, Ward SM. Nitric oxide and its role as a non-adrenergic, non-cholinergic inhibitory neurotransmitter in the gastrointestinal tract. British Journal of Pharmacology. 2019; 176: 212–227. https://doi.org/10.1111/bph.14459.

[28] Uwada J, Yazawa T, Islam MT, Khan MRI, Krug SM, Fromm M, *et al*. Activation of muscarinic receptors prevents TNF-$\alpha$-mediated intestinal epithelial barrier disruption through p38 MAPK. Cellular Signalling. 2017; 35: 188–196. https://doi.org/10.1016/j.cellsig.2017.04.007.

[29] Uwada J, Nakazawa H, Muramatsu I, Masuoka T, Yazawa T. Role of Muscarinic Acetylcholine Receptors in Intestinal Epithelial Homeostasis: Insights for the Treatment of Inflammatory Bowel Disease. International Journal of Molecular Sciences. 2023; 24: 6508. https://doi.org/10.3390/ijms24076508.

[30] Xiao S, Li Q, Hu L, Yu Z, Yang J, Chang Q, *et al*. Soluble Guanylate Cyclase Stimulators and Activators: Where are We and Where to Go? Mini Reviews in Medicinal Chemistry. 2019; 19: 1544–1557. https://doi.org/10.2174/1389557519666190730110600.

[31] Bose A, Visweswariah SS. Gut reactions and gut instincts: regulation of intestinal homeostasis by receptor guanylyl cyclase C (GC-C). The Biochemical Journal. 2025; 48: BCJ20253055. https://doi.org/10.1042/BCJ20253055.

[32] Yamamoto Y, Okano T, Yamada H, Akashi K, Sendo S, Ueda Y, *et al*. Soluble guanylate cyclase stimulator reduced the gastrointestinal fibrosis in bleomycin-induced mouse model of systemic sclerosis. Arthritis Research & Therapy. 2021; 23: 133. https://doi.org/10.1186/s13075-021-02513-y.

[33] Hong Y, Boiti A, Vallone D, Foulkes NS. Reactive Oxygen Species Signaling and Oxidative Stress: Transcriptional Regulation and Evolution. Antioxidants (Basel, Switzerland). 2024; 13: 312. https://doi.org/10.3390/antiox13030312.

[34] Checa J, Aran JM. Reactive Oxygen Species: Drivers of Physiological and Pathological Processes. Journal of Inflammation Research. 2020; 13: 1057–1073. https://doi.org/10.2147/JIR.S275595.

[35] Stavely R, Ott LC, Rashidi N, Sakkal S, Nurgali K. The Oxidative Stress and Nervous Distress Connection in Gastrointestinal Disorders. Biomolecules. 2023; 13: 1586. https://doi.org/10.3390/biom13111586.

[36] Vona R, Pallotta L, Cappelletti M, Severi C, Matarrese P. The Impact of Oxidative Stress in Human Pathology: Focus on Gastrointestinal Disorders. Antioxidants (Basel, Switzerland). 2021; 10: 201. https://doi.org/10.3390/antiox10020201.

[37] Tawa M, Okamura T. Factors influencing the soluble guanylate cyclase heme redox state in blood vessels. Vascular Pharmacology. 2022; 145: 107023. https://doi.org/10.1016/j.vph.2022.107023.

[38] Shah RC, Sanker S, Wood KC, Durgin BG, Straub AC. Redox regulation of soluble guanylyl cyclase. Nitric Oxide: Biology and Chemistry. 2018; 76: 97–104. https://doi.org/10.1016/j.niox.2018.03.013.

[39] Sandner P, Zimmer DP, Milne GT, Follmann M, Hobbs A, Stasch JP. Soluble Guanylate Cyclase Stimulators and Activators. Handbook of Experimental Pharmacology. 2021; 264: 355–394. https://doi.org/10.1007/164_2018_197.

[40] Liu R, Kang Y, Chen L. Activation mechanism of human soluble guanylate cyclase by stimulators and activators. Nature Communications. 2021; 12: 5492. https://doi.org/10.1038/s41467-021-25617-0.

[41] Stuehr DJ, Misra S, Dai Y, Ghosh A. Maturation, inactivation, and recovery mechanisms of soluble guanylyl cyclase. The Journal of Biological Chemistry. 2021; 296: 100336. https://doi.org/10.1016/j.jbc.2021.100336.

[42] Wang Y, Wang L, Zhang H, Ren P, Cheng X, Hong F, *et al*. Immunostimulatory effects mechanism of polysaccharide extracted from Acanthopanax senticosus on RAW 264.7 cells through activating the TLR/MAPK/NF-κB signaling pathway. Scientific Reports. 2025; 15: 13440. https://doi.org/10.1038/s41598-025-97423-3.

[43] Tian H, Ling N, Guo C, Gao M, Wang Z, Liu B, *et al*. Immunostimulatory activity of sea buckthorn polysaccharides via TLR2/4-mediated MAPK and NF-κB signaling pathways in vitro and in vivo. International Journal of Biological Macromolecules. 2024; 283: 137678. https://doi.org/10.1016/j.ijbiomac.2024.137678.

[44] Fan AA. Structural Analysis and Biological Activity of Polysaccharides from the Roots and Rhizomes of Megacarpaea delavayi [Master's Thesis]. Dali University: Dali. 2020. (In Chinese)